ACTIVE VIBRATION CONTROL USING PID-AFC CONTROLLER OF THE PIEZO STACK ACTUATOR WITH CONSIDERATION TO HYSTERESIS AND SATURATION EFFECTS

Ahmad Zhafran Ahmad Mazlan*, Zaidi Mohd Ripin and Wan Mohd Amri Wan Mamat Ali

TheVibrationLab, School of Mechanical Engineering, Universiti Sains Malaysia, MALAYSIA
email: zulryan_85@yahoo.com*

Analysis of the active vibration control (AVC) system is made with consideration to the non-linear hysteresis and saturation of the piezo stack actuator. The AVC system is subjected to the base excitation which included the rotating unbalanced mass and the friction induced force as the disturbance to the system. The piezo stack actuator non-linear characteristics are measured and included in the model of the actuator of the AVC system. Two types of controller are designed for comparison which is Proportional-Integral-Derivative (PID) and Active Force Control (AFC) to attenuate the transmitted vibration from the base to the structure. The effectiveness of both controllers in dealing with the non-linear hysteresis and saturation of the piezo stack actuator are compared. The result shows that, the PID-AFC controller can reduced the vibration of the system by 97.7 % compared to the PID controller with 89.3 % of vibration attenuation. This result proved that, the PID-AFC controller is more effective and robust for the AVC systems even though under the influence of the non-linear hysteresis and saturation of the piezo stack actuator.

Keywords: Active vibration control, piezo stack actuator, hysteresis, saturation, PID-AFC

1. Introduction

Piezoelectric materials are capable of converting the mechanical stress to the electrical charge and vice versa. These piezoelectric effects made them useful for sensors and actuators in many applications, such as in control of structural vibration [1]. Nonlinear hysteresis and saturation are inherent characteristics of the piezoelectric actuator which affect their performance. The hysteresis of the piezoelectric actuator has been widely studied and the effect can be compensated using their inverse models [2]. However, for the saturation effect, there is no specific study has been carried out for the piezoelectric actuator. Both hysteresis and saturation characteristics are important, in particular for developing the active vibration control (AVC) system using the piezoelectric actuator. AVC using the piezoelectric actuator has been widely studied in reducing the vibration of structures, such as flexible beam [3], but rarely been studied for the power tool application. The piezoelectric actuator of the AVC system can be controlled using various control techniques, such as sliding mode [4] and Proportional-Integral-Derivative (PID) control [5]. The voltage supplied to the PID control can be saturated based on the limitation of the amplifier and the actuator.

Active Force Control (AFC) is one of the control techniques which have been widely used for the AVC applications. It was introduced by Hewit and Burdess in year 1981 for the robotic application and nowadays is used in various fields such as automotive [6] and flexible structure [3] applications. AFC has been proved as one of the effective control scheme for the AVC system, even when under the influence of various disturbances and conditions. For example in automotive application, the skyhook and adaptive neuro AFC was developed to control the pneumatic actuator of the vehicle active suspension system and the results show that, the proposed AFC scheme has a better performance for mass acceleration with 30 % of amplitude reduction compared to the PID controller [6]. Even though there are a lot of studies on the AFC application, the effectiveness of the AFC in dealing with piezoelectric actuator hysteresis and saturation has not been reported in the literature. This study considers the application of the AFC, in order to investigate its effectiveness for the active suspended handle model with the presence of piezoelectric actuator hysteresis and saturation effects.

2. Methodology

2.1 Piezo stack actuator characterization

In this study, the hysteresis and saturation of the piezo stack actuator (PI type P-010.00) is investigated in terms of force and voltage as a relationship of excitation frequency. Fig. 1 shows the schematic diagram and photograph of the piezo stack actuator characterization. In the figure, a sine wave voltage signal from 100 to 500 Hz with a step up voltage from 1 to 5 V is generated by the LabVIEW software to the NI 9263 output module. The voltage is then amplified by the high voltage piezo amplifier (PI type E-508.00) to excite the piezo stack actuator. The dynamic force is measured by the load cell (Kistler type 9272) and the signal is captured using the data acquisition (iMC device) and sent to the computer with iMC software for data analysis. From this measurement, the hysteresis and saturation characteristics of the piezo stack actuator can be determined.

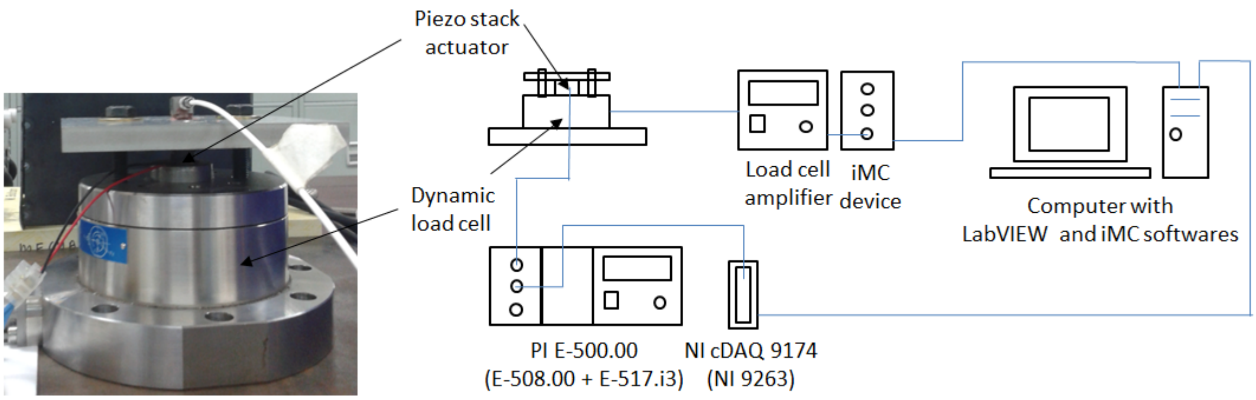

Figure 1: Schematic diagram and photograph of the piezo stack actuator characterization.

2.2 Vibration measurement of die-grinder

In this study, the input spectrum of the die grinder is used as disturbance $F_d(t)$ to the AVC system. For the input spectrum measurement, an accelerometer is mounted at the front body of the die-grinder to the measure the acceleration in three conditions; (a) without collet, (b) with collet and (c) grinding on the mild steel plate. This measurement includes the effect of unbalanced mass (collet) $N_x(t)$ and friction induced force $F_r(t)$ as shown in the following equation:

$$F_d(t) = (N_x + F_r)(t) \tag{1}$$

The accelerometer signal obtained from the die grinder is connected to the NI 9234 input module with the integration of LabVIEW software for data analysis.

2.3 Mobility measurement of suspended handle

In this study, an active suspended handle [7] is used as an AVC system. The mobility measurement is carried for the suspended handle to obtain the frequency response function (FRF) including the dynamic mass, damping and stiffness for the modelling of the suspended handle. This measurement using the LMS Test Lab software consists of the instrumentation such as impact hammer (Kistler type 9724A500), accelerometer (Kistler type 8776A50) and data acquisition LMS SCADAS.

2.4 Development of active suspended handle model with PID and AFC controllers

Fig. 2 shows the single-degree-of-freedom (SDOF) model of an active suspended handle which subjected to the base excitation from the die-grinder.

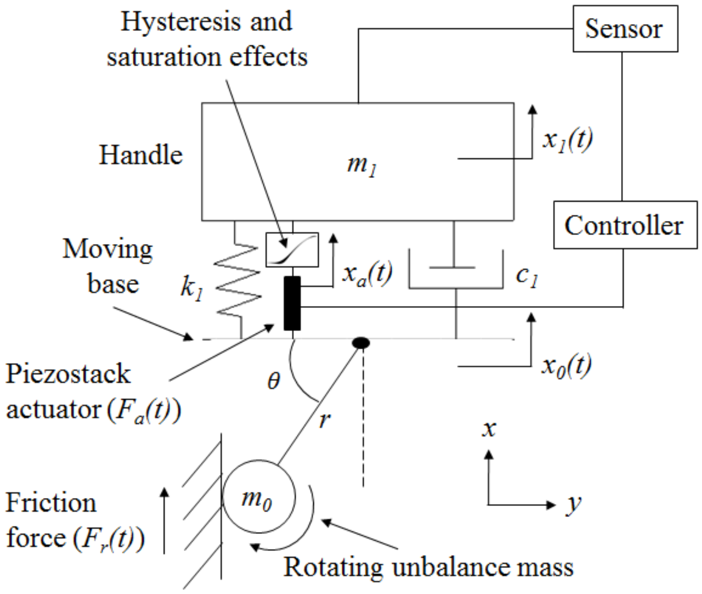

Figure 2: Model of the active suspended handle with hysteresis and saturation effects.

In this figure, the model of the active suspended handle is based on the parallel type coupled piezo actuator-structure, where the actuator is mounted between the handle and the moving base [8]. The equation of motion of the active suspended handle which subjected to the base excitation from the die-grinder can be written as follows:

$$m_1\ddot{x}_1(t) + c_1(\dot{x}_1 - \dot{x}_0)(t) + k_1(x_1 - x_0)(t) = F_a(t) \tag{2}$$

where, m_1, c_1 and k_1 are the dynamic mass, damping and stiffness of the handle. The sensor measures the handle acceleration $\ddot{x}_1(t)$ and sent the signal to the controller. The feedback signal from the controller is used to generate the counter force $F_a(t)$ of the piezo stack actuator to compensate the disturbance from the moving base $x_0(t)$. The relationship between the applied voltage $V_a(t)$ and the actuating force $F_a(t)$ of the piezo stack actuator with the consideration to hysteresis and saturation nonlinearity effects can be written as follows:

$$F_{a\,sat}(t) = (\alpha + \Delta\alpha)_{(V,\omega)}V_{a\,sat}(t) \tag{3}$$

where, $\alpha_{(V,\omega)}$ is the proportional constant and $\Delta\alpha_{(V,\omega)}$ is the deviation part (i.e., hysteresis effect) of piezo stack actuator. These parameters can be experimentally determined and both are voltage and frequency dependent [4, 7]. From Eq. (3), the piezo stack actuating force is subjected to the saturation voltage $V_{a\,sat}(t)$. This occurred when the displacement differences of the handle and base $x_1(t) - x_0(t)$ is equal or exceed the actuator maximum stroke $x_{a\,sat}(t)$ as follows:

$$x_{a\,sat}(t) \leq x_1(t) - x_0(t) \tag{4}$$

In order to design the controller of the active suspended handle, the state-space model must be shown. By including Eq. (3) into Eq. (2), the components of spate-space model are derived as follows:

$$\mathbf{x}(t) = [x_1 \quad \dot{x}_1]^T,\ \mathbf{u}(t) = [0 \quad F_{a\,sat}],\ \mathbf{d}(t) = [0 \quad c_1\dot{x}_0 + k_1x_0],$$

$$\mathbf{A} = \begin{bmatrix} 0 & 1 \\ -\frac{k_1}{m_1} & -\frac{c_1}{m_1} \end{bmatrix},\ \mathbf{B} = \begin{bmatrix} 0 \\ \frac{1}{m_1} \end{bmatrix},\ \mathbf{\Gamma} = \begin{bmatrix} 0 \\ \frac{1}{m_1} \end{bmatrix},\ \mathbf{C} = [0 \quad 1] \tag{5}$$

where, **A** is the system matrix, **x**(t) is the state vector, **B** is the input matrix, **u**(t) is the control input, **Γ** is the disturbance matrix, **d**(t) is the system disturbance and **C** is the output matrix of the measured mass acceleration [8].

In this study, two types of controller are developed; PID and AFC controllers [5, 9]. The voltage V_a feed to the piezo stack actuator from each controller can be derived as follows:

a) PID controller

$$V_{a\,PID}\,(t) = K_P\,(x_r - x_1)(t) + K_I \int (x_r - x_1)(t)dt + K_D\, d(x_r - x_1)(t)/dt \tag{6}$$

b) AFC controller

$$V_{a\,AFC}\,(t) = k_{AFC}\left(\frac{F_{a\,sat} - M^*\ddot{x}_1}{(\alpha + \Delta\alpha)_{(V,\omega)}}\right)(t) \tag{7}$$

where, K_P, K_I and K_D are the proportional, integral and derivative constants, $e(t) = x_r(t) - x_1(t)$ is the error signal of desired output $x_r(t)$ to the handle displacement $x_1(t)$, k_{AFC} is the AFC percentage constant and M^* is the estimated mass [9]. Basically, the combination of PID-AFC controller can produced a better counter voltage to the piezo stack actuator, with the respect to the saturation voltage $V_{a\,sat}(t)$. Thus, by including Eq. (6) and (7) into Eq. (2), the active suspended handle with PID-AFC controller can be rewritten as Eq. (8) and the overall block diagram is shown in Fig. 3.

$$m\ddot{x}_1(t) + c(\dot{x}_1 - \dot{x}_0)(t) + k(x_1 - x_0)(t) = (\alpha + \Delta\alpha)_{(V,\omega)}\,\{\,(K_P\,(x_r - x_1)(t) + K_I \int (x_r - x_1)(t)dt + K_D\, d(x_r - x_1)(t)/dt) + \left(k_{AFC}\left(\frac{F_a - M^*\ddot{x}_1}{(\alpha + \Delta\alpha)_{(V,\omega)}}\right)(t)\right)\} \tag{8}$$

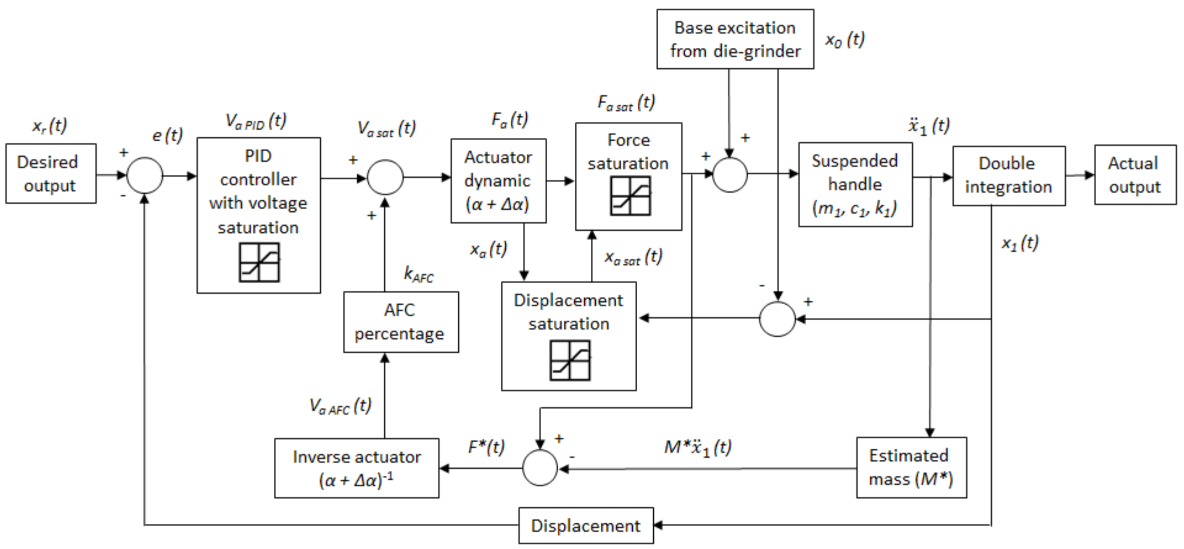

Figure 3: AVC block diagram of the active suspended handle with a PID-AFC controller.

3. Results and discussion

3.1 Piezo stack actuator hysteresis and saturation effects

Fig. 4 shows the result of the piezo stack actuator forces at different operating frequencies and voltages.

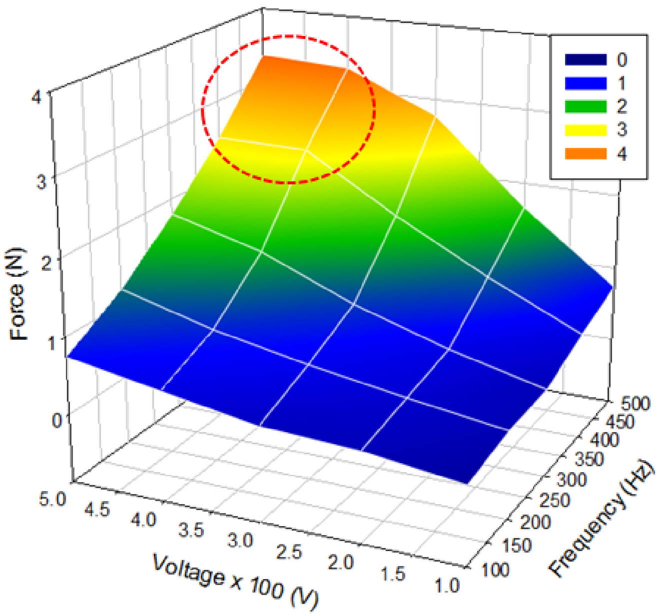

Figure 4: Measured hysteresis and saturation characteristics of the piezo stack actuator.

From the figure, the force of the piezo stack actuator at each operating frequency increased proportional to the supplied voltage of 100 - 500 V. The hysteresis of the piezo stack actuator can be observed at each operating frequency where there is a non-linearity effect $\Delta\alpha_{(V,\omega)}$ at the voltage-force curve. For the frequency of 100 - 300 Hz, the piezo stack actuator did not face saturation while for frequency of 400 Hz and 500 Hz, the force saturation occurred at 400 V as highlighted in Fig. 4. From the figure, the piezo stack actuator voltage-force relationship with hysteresis and saturation effects in Eq. (3) can be frequency dependent written as follows:

$$F_{a\,100}(t) = (0.018V_{ai}^{\,2} + 0.048V_{ai} + 0.06)(t)$$

$$F_{a\,200}(t) = (0.024V_{ai}^{\,2} + 0.088V_{ai} + 0.134)(t)$$

$$F_{a\,300}(t) = (0.012V_{ai}^{\,2} + 0.329V_{ai} - 0.102)(t)$$

$$F_{a\,400}(t) = (0.038V_{ai}^{\,2} + 0.465V_{ai} + 0.018)(t)$$

$$F_{a\,500}(t) = (-0.103V_{ai}^{\,2} + 1.392V_{ai} + 0.588)(t) \tag{9}$$

where, i = 1, 2, .., 5 is an increment of the supplied voltage. For the case of frequency 400 Hz and 500 Hz, both hysteresis and saturation characteristics are considered whereby the force $F_{a\,400}$ and $F_{a\,500}$ are saturated at V_{ai} = 400 V. For frequencies below 300 Hz, only hysteresis characteristic is considered for the piezo stack actuator.

3.2 Vibration spectrum of die-grinder

Fig. 5 shows the input spectrum (acceleration) of the die grinder in the vertical axis direction. For the case of operating without collet, the acceleration of the front body of the die grinder is 19.4 m/s^2 at the operating frequency of 445 Hz. By including the collet, the acceleration of the front body increased to 24.3 m/s^2. The acceleration of the grinder shows the significant increment to 85.3 m/s^2 when grinding on the mild steel plate with a reduction of operating frequency to 417 Hz. This is due to the effect of friction induced force F_r and the resistance of the work-piece which slowing the motor when grinding on the mild steel plate.

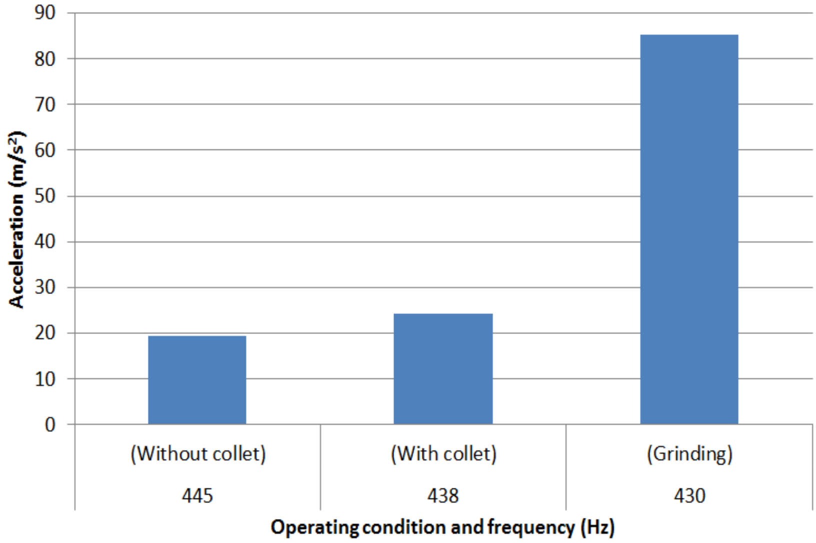

Figure 5: Input spectrum of the die grinder in three conditions; (a) without collet, (b) with collet and (c) grinding on the mild steel plate

3.3 Model validation

Fig. 6 shows the comparison between the experimental and model FRF of the active suspended handle. From the figure, there are two peaks (natural frequencies) at 238 Hz and 491 Hz. The 2nd natural frequency of 491 Hz has a higher mobility output compared to the 1st natural frequency of the handle. Thus, the point mobility at 491 Hz is extracted from the model FRF to calculate the dynamic mass, damping and stiffness of the active suspended handle model. From Fig. 6, it also realized that the model FRF is in agreement with the experimental FRF.

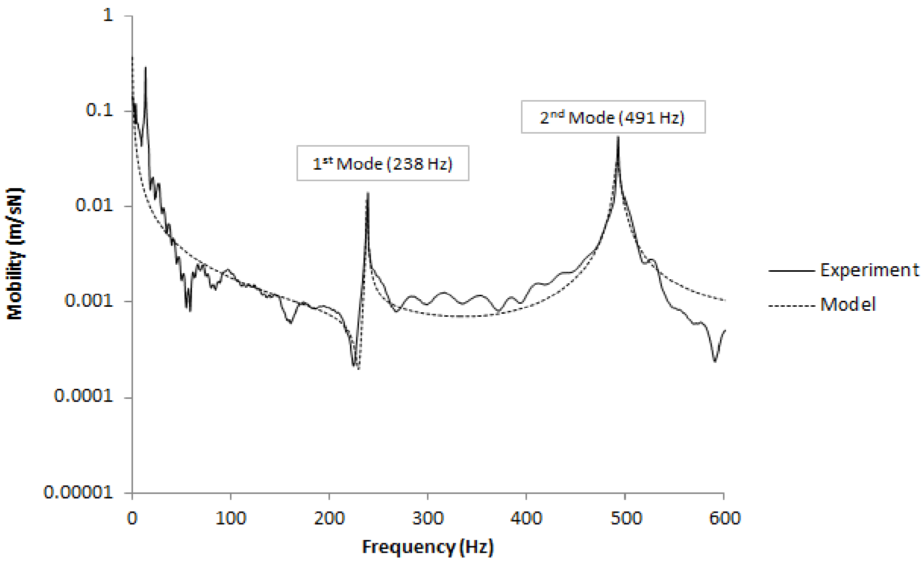

Figure 6: Experimental and model FRF of the active suspended handle

3.4 PID and AFC controller performances

For the AVC system with PID controller in Eq. (6), a continuous type-PID controller is used with an advance function of voltage saturation and auto-tuning method is applied for the tuning of

PID controller. From the tuning, an optimum P, I and D parameters are obtained as P = 87.09, I = 23948 and D = 0.0225. For the AVC system with AFC controller in Eq. (7), a crude-approximation (CA) tuning method is applied with the consideration to piezo stack actuator hysteresis and saturation effects. Fig. 7 shows the handle displacement overshoot percentage of the different estimated mass values. From the figure, it is observed that the higher estimated mass values, the worse overshoots were occurred. For example, the highest estimated mass value of 2 kg produced the highest displacement overshoot of 62.4 %. From this *M** parameters analysis, the lowest displacement overshoot was achieved when the *M** = 0.1 kg with 8.4 % of displacement overshoot. Further reduction of the estimated mass values, such as *M** = 0.01 kg - 0.001 kg gives no effect to the reduction of the displacement overshoot percentage. From these results, the optimum estimated mass value for the active suspended handle model is decided as 0.1 kg.

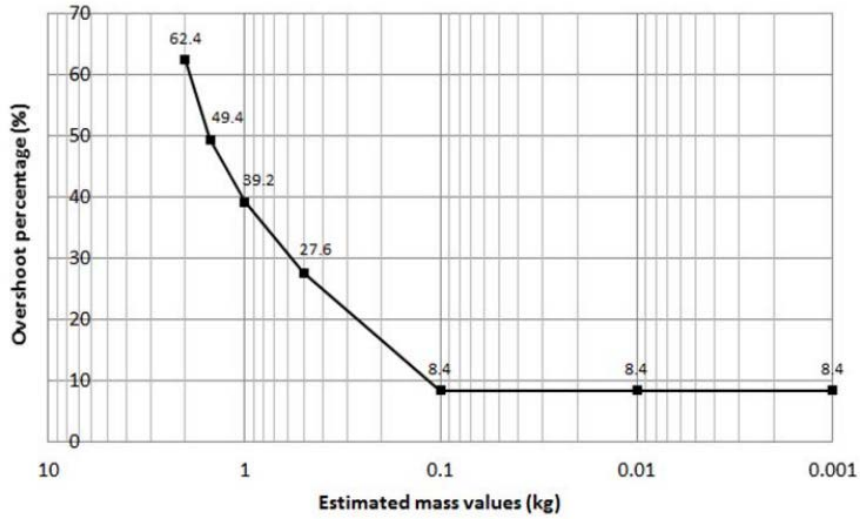

Figure 7: Displacement overshoot percentage of different estimated mass values

Fig. 8 shows the frequency response of the acceleration between the PID and PID-AFC controllers of the active suspended handle model. From the figure, the acceleration of the model with a PID-AFC controller produced the output acceleration of 1.92 m/s^2 at the operating frequency 430 Hz, which is 97.7 % of vibration reduction compared to the model with PID controller with 8.22 m/s^2, 89.3 % of vibration reduction from the die-grinder acceleration of 85.3 m/s^2. This result proved that the PID-AFC controller is more effective and robust for the AVC systems even though under the influence of the non-linear hysteresis and saturation of the piezo stack actuator.

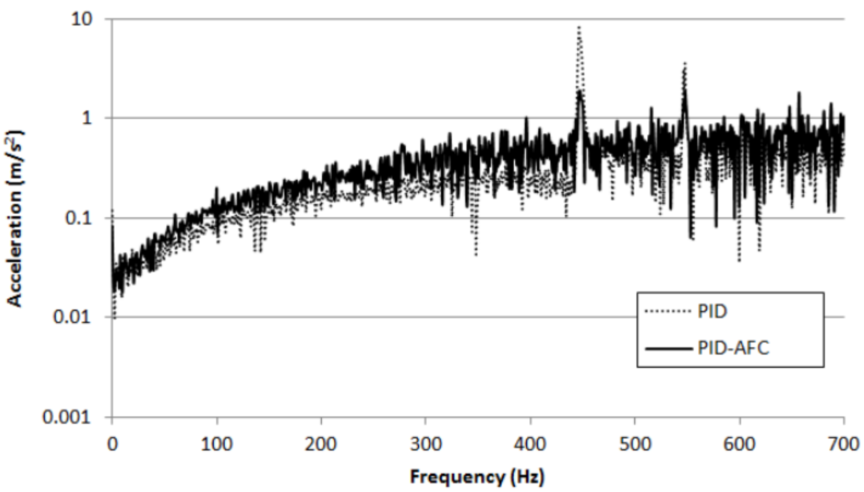

Figure 8: Acceleration frequency response between the PID controller and PID-AFC controller

4. Conclusions

From this study, the target to build the AVC system (active suspended handle) using the PID and PID-AFC controllers with the consideration of piezo stack actuator hysteresis and saturation effects have been achieved. The results show that, the AVC system with the PID-AFC controller is more effective in reducing the vibration from the die-grinder compared to the PID controller even though under the influence of piezo stack actuator hysteresis and saturation effects.

5. Acknowledgement

This project was funded by the Universiti Sains Malaysia through the TPLN grant (302/JPNP/312001) and Short-Term grant (304/PMEKANIK/60313052).

REFERENCES

1 Tuma, J., Šimek, J., Škuta, J. and LOS, J. Active Vibrations Control of Journal Bearings with the Use of Piezoactuators, *Mechanical Systems and Signal Processing,* 36**,** 618-629, (2013).

2 Wang, G., Guan, C., Zhou, H., Zhang, X. and Rao, C. Hysteresis Compensation of Piezoelectric Actuator for Open-loop Control, *Chinese Optics Letters,* 11**,** 21202-1-4, (2013).

3 Maslan, M. N., Mailah, M. and Mat Darus, I. Z. Identification and Control of a Piezoelectric Bender Actuator, *Proceedings of the 3rd International Conference on Intelligent Systems, Modelling and Simulation*, 8-10 Feb., (2012).

4 Nguyen, V.-Q., Choi, S.-M., Han, Y.-M., Choi, S.-B. and Moon, S.-J. The Design of a Piezostack-based Active Mount and Application to a Vibration Control System, *Smart Materials and Structures,* 17**,** 065029-1-9, (2008).

5 Jovanovic, M. M., Simonovic, A. M., Zoric, N. D., Lukic, N. S., Stupar, S. N. and Ilic, S. S. Experimental Studies on Active Vibration Control of a Smart Composite Beam Using a PID Controller, *Smart Materials and Structures,* 22, 115038-1-8, (2013).

6 Priyandoko, G., Mailah, M. & Jamaluddin, H. Vehicle Active Suspension System Using Skyhook Adaptive Neuro Active Force Control, *Mechanical Systems and Signal Processing,* 23**,** 855-868, (2009).

7 Mazlan, A. Z. A. and Ripin, Z. M. The Effective Frequency Range of an Active Suspended Handle Based on the Saturation Effects of a Piezo Stack Actuator, *Journal of Vibration and Control*, 1077546315585218, (2015).

8 Choi, S., Seong, M., Ha, S., Jeon, J. and Sohn, J. Design of a Piezostack-based Inertial Actuator and Application to Vibration Control: Experimental Investigation, *Proceedings of the Institution of Mechanical Engineers, Part I: Journal of Systems and Control Engineering,* 225**,** 1115- 1124, (2011).

9 Al-Mola, M. H., Mailah, M., Kazi, S., Muhaimin, A. H. and Abdullah, M. Y. Robust Active Force Controller for an Automotive Brake System. *Proceedings of the 3rd International Conference on Intelligent Systems, Modelling and Simulation*, 8-10 Feb., (2012).